

Cold plasma enamel surface treatment to increase fluoride varnish uptake

S. Fathollah

Amirkabir University of Technology

H. Abbasi (✉ abbasi@aut.ac.ir)

Amirkabir University of Technology

S. Akhoundi

Tehran University of Medical Sciences

A. Naeimabadi

Amirkabir University of Technology

S. Emamjome

Tehran University of Medical Sciences

Research Article

Keywords: Helium-DBD jet, Argon jet, Air-DBD, Dental Care, Fluoridation, Tooth remineralization

Posted Date: September 23rd, 2021

DOI: <https://doi.org/10.21203/rs.3.rs-842386/v1>

License:   This work is licensed under a Creative Commons Attribution 4.0 International License.

[Read Full License](#)

Version of Record: A version of this preprint was published at Scientific Reports on March 18th, 2022. See the published version at <https://doi.org/10.1038/s41598-022-08069-4>.

Cold plasma enamel surface treatment to increase fluoride varnish uptake

S. Fathollah^a, H. Abbasi^{a,*}, S. Akhondi^{b,c}, A. Naeimabadi^a, and S. Emamjome^c

^aFaculty of Physics and Energy Engineering, Amirkabir University of Technology,

P. O. Box 15875-4413, Tehran, Iran

^bDental Research Center, Dentistry Research Institute, Tehran University of Medical Sciences, Tehran, Iran

^cDepartment of Orthodontics, School of Dentistry, Tehran University of Medical Sciences, Tehran, Iran

*corresponding author

Abstract

Enamel strengthening to prevent the first stage of caries has been an essential issue in oral health recently. Among the available methods to increase enamel strength, fluoride varnish treatment has relatively better results in preventing tooth decay. Cold plasma capabilities in sterilizing the environment, surface modification, and improving adhesion are well known. Accordingly, this study aims to increase the enamel layer's adhesion hoping that the intensity and time of enamel interaction with FV and the absorption of fluoride ions will increase. Accordingly, we randomly divided twenty bovine teeth into two groups A (consisting of four teeth) and B (composed of four subgroups, each containing four teeth). Samples of group A and one specimen of each subset B investigate the effect of using Helium-DBD (He-DBDJ), Argon (ArJ), and Air-DBD jet on the enamel surface. Other B specimens are devoted to the study of the release of FV fluoride ions from processed enamel. The scanning electron microscope (SEM) images show that although ArJ and Air-DBD have significantly damaged the enamel's hexagonal structures, they are only changed from convex to concave in the He-DBDJ case. For this reason, enamel effectively enhances the capacity to accept more FV. The energy-dispersive X-ray spectroscopy (EDX) indicates an increase in calcium ratio to

phosphorus and the amount of fluoride and sodium absorption in the enamel layer in processing with He-DBDJ plasma. The latter helps restore the damaged parts of the enamel. Analysis of fluoride released from the FV did not show a significant change owing to plasma processing. The combination of Cold plasma and varnish fluoride on treatment enamel could be unique ability to improve reinforcement of tooth enamel against of tooth decay.

Keywords: Helium-DBD jet, Argon jet, Air-DBD, Dental Care, Fluoridation, Tooth remineralization

1. Introduction

There are several factors involved in dental caries and related infections. Numerous studies and research in the last few decades in preventing tooth decay show that it is still the most chronic disease in primary school children [1, 2]. Minerals are absorbed and excreted from the enamel every day. Tooth decay occurs due to carbohydrate metabolism in bacteria in the mouth and a lower pH level than the critical value ($\text{pH} = 5.5$), which leads to a change in the concentration of calcium and phosphate ions in saliva. The acid produced by bacteria dissolves the enamel surface and then the dentin [3-5]. Today, in addition to the strict recommendation for proper and regular oral hygiene, the use of fissure sealants, systemic and topical fluoride, and diet control have also been suggested as complementary methods to prevent tooth decay. Because fluoride is less likely to be absorbed and the toothbrush has less access to microbial plaque in these areas, fissure sealant the holes and crevices [6, 7]. Fluoride can prevent tooth decay in three ways. First, fluoride can be easily absorbed systemically (through milk, food, and water) and transferred to the enamel during the pre-eruptive period of tooth formation^{8,9}. As a result, the fluoride ion replaces the OH bond in the hydroxyapatite crystal and forms a crystal. In terms of rot resistance, fluorapatite is much more resistant than hydroxyapatite. Topical fluoride causes tooth strength. Moreover, it can accelerate remineralization and prevent tooth surface demineralization after tooth eruption [8-10]. Besides, topical fluoride makes bacteria more vulnerable to acid by stopping the glycolysis process in the microorganism [11].

There are several ways to apply topical fluoride to the tooth surface. Topical fluoride in the form of 2 % sodium fluoride, 1.23 % APF gel, and FV is the most common fluoride therapy method in dental clinics [12-16]. The fluoride in these methods creates a physical barrier against acid restriction by forming a sedimentary layer of calcium fluoride on the enamel and improving tooth enamel structure by creating a fluoride storage source. Numerous studies show that FV is superior to other forms due to its ease of use, especially for children, saving time, and the rare possibility of fluoride ingestion. However, topical fluoride dissolves in the presence of an acid, so its protective ability is limited. Therefore, fluoride therapy needs to be repeated at regular intervals [17-20]. As a result, increasing the effect of fluoride coating and its durability with appropriate fluoride concentrations is still a significant challenge for researchers in this field. In this regard, the use of laser radiation [21-23] ozone therapy [24, 25], and photodynamic therapy [26] have been tested in this respect, although still, are not reliable.

The situation described has coincided with a plasma technology development stage that provides plasma access with two main features: atmospheric pressure and body temperature, known as cold-atmospheric pressure plasma, abbreviated CAP. Based on the mentioned features, CAP technology has been the source of numerous medical field experiments that have yielded brilliant and thought-provoking results. Due to the wide range of CAP medical applications, we avoid going into details and refer those interested to a few references for further studies [27-31]. However, let us mention some of the research related to plasma dentistry applications: plasma introduces applications in pathogens removal in bacterial plaque, tooth bleaching, bond strength, endodontic therapy, and increasing hydrophilicity [32-36].

Among the CAP-derived effects that led us to design a research stream to strengthen tooth enamel is CAP's ability to change the surface's physical and chemical properties that CAP has processed. In other words, using CAP can be expected to alter i) the properties of hydrophilicity and hydrophobicity ii) change the electrical properties of the enamel surface and thus change the surface adsorption capacity iii) change the structure of some bonds in the surface area by replacing some units in the surface structure either by CAP-derived radicals or replacement by the other agents mediated by these radicals. Accordingly, the idea that

adequate processing of the enamel surface with a type of CAP could increase fluoride ion uptake and its replacement by OH bond in hydroxyapatite was worth trying. The process leads to fluorapatite formation with a stiffer structure and resistance to destructive factors and erosion. Although this dream seems achievable, its realization requires sufficient knowledge of the physical and chemical factors involved, which is possible through the design and conduct of numerous experiments.

To give an idea of the challenges ahead, we should address two main issues, the unknown plasma-enamel interaction and the diversity in the architecture of existing plasma systems. The degrees of freedom associated with both problems diversify the possible scenarios to such an extent that it is challenging to decide on the appropriate strategy. Accordingly, the pilot phase was defined to be as comprehensive as possible and, at the same time, limited to a few parameters. The analysis of the pilot results provides a degree of cognition for the choice of preferred architecture. Keep in mind that preferred architecture makes sense in fluoride uptake and minor damage caused by plasma processing to the enamel structure. Based on this, three types of helium, argon, and air are the working gas for plasma systems with three different discharge reactor designs. Figure 1 shows a schematic of the plasma architectures used in this study.

This article shows that we are still far from reaching the destination despite the considerable evidence showing the correct orientation and movement towards the goal. Other experiments are needed to clear up the ambiguities.

2. Materials and Methods

2.1. Enamel Specimens Preparation

We use twenty extracted bovine incisors from an abattoir in this investigation. All the methods were carried out in accordance with relevant guidelines. The guidelines are approved by Research Committee (IR.TUMS.VSR.REC.1397.757) of Tehran University of Medical Sciences. On behalf of the Tehran

University of Medical Sciences, the mentioned bovine teeth were ordered to the Tehran Slaughter Center, responsible for slaughtering cows to supply Tehran's meat under the supervision of the Ministry of Health and Medical Education. Under the personal supervision of the Tehran University, Slaughterhouse officials extracted out the bovine's teeth immediately after slaughtering the animals. Care was taken to select the newly extracted teeth to be completely healthy (without decay) and immediately immersed in a 0.05% chloramine solution at 4°C for four days to maintain their moisture and avoid environmental contamination. The first step in preparing the selected teeth was to thoroughly clean the soft tissues left on them with pumice slurry and hand scale. The next step was to cut the cementum enamel with a low-speed water-cooled diamond saw. Next, a 10X stereomicroscope examined all samples' buccal surfaces to ensure the quality of cleanliness, absence of structural defects, and micro-fracture for removing unsuitable specimens from the collection. Then, we fixed the final 20 samples in molds containing acrylic resin so that their buccal surface is upwards. Finally, they were coated with two layers of protective nail varnish to cover the enamel area leaving a treatment window of approximately 2×4 mm. At all sample preparation stages, their storage environment's humidity and temperature were 95% and 25°C, respectively.

2.2. Specimens Grouping

After preparing twenty samples and passing them through the final stage of quality control, we randomly divided them into two groups A (consisting of four teeth) and B (including sixteen teeth). We have introduced group A exclusively to study changes in enamel surface due to plasma processing. For this purpose, we first process the enamel surface of three A group samples by Helium Dielectric Barrier Discharge Jet (He-DBDJ), Argon Jet (ArJ) Air-DBD. Then, compare the processed specimens with the remaining A group member, i.e., control (C). Group B, consisting of sixteen teeth in four subgroups, is assigned to a scenario in which the three subgroups' treated teeth (by three plasma devices) and the remaining subgroup's unprocessed teeth are impregnated with FV. We have identified the symbols He-

DBDJ + FV, ArJ + FV, Air-DBD + FV, and C + FV at the end of this step. We use one tooth from each of these subgroups for Scanning Electron Microscope [34] imaging and the other teeth to measure fluoride ion uptake. Figure 1 shows schematic images of each of the plasma devices used in this study.

2.3. Topical Fluoride Application

The enamel slabs were thoroughly rinsed with distilled water and delicately dried with a towel. As mentioned earlier, group A is only affected by plasma processing without receiving FV. In contrast, on the surface of Group B samples, after processing by plasma, a layer of FV containing 5% sodium fluoride (Oratech, USA) with a thickness of 2 mm (weighing 0.1 g) is placed by micro brush. According to the manufacturer's recommendation, after impregnating the samples with FV, the samples were exposed to dry air for 2 minutes to reduce the FV's moisture content. Finally, we simulate the oral environment by immersing the teeth in 37°C distilled water.

2.4. CAP Devices

Along with our curiosity about how and to what extent cold-atmospheric pressure plasma affects fluoride ion adsorption in enamel, the variation in geometry and details of the mechanism and parameters involved in the electrical discharge process make the choice of the "appropriate architecture" for this treatment a fundamental question. We nominate three relatively different architectures from different strategies that could lead to selecting the appropriate architecture. We believe overlapping their features can lead to a minimum of knowledge necessary to choose the desired device. Accordingly, to better examine the results and their analysis, it must provide a clear picture of the plasma devices' geometry and characteristics in this research. Figure 1 schematically shows the three plasma generators.

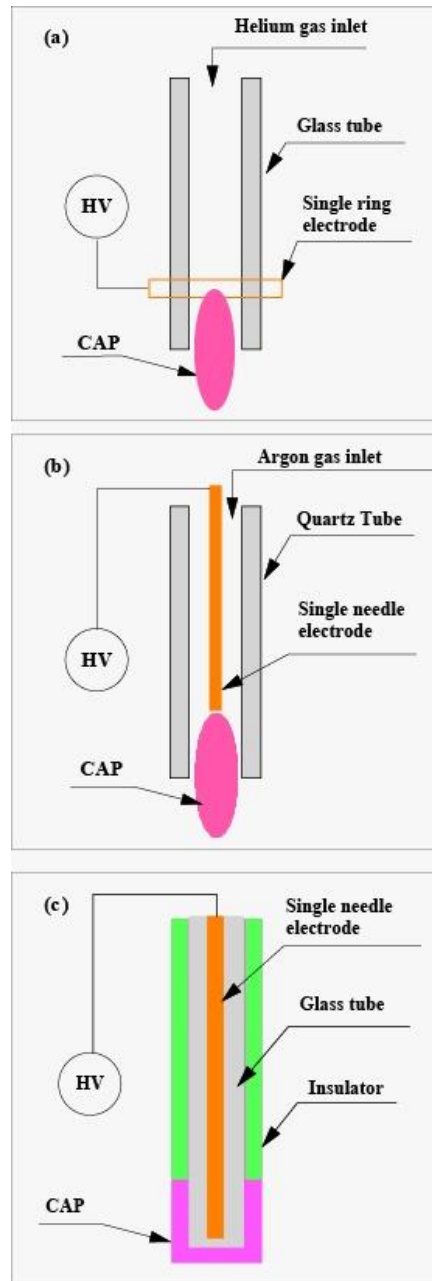


Fig. 1 - Schematic of cold-atmospheric pressure plasma devices used for enamel processing a) He-DBDJ b) ArJ c) Air-DBD.

Figure 1a shows a He-DBDJ whose main body is a glass cylinder, and helium gas is injected into one of its two ends into the cylinder, resulting in a steady flow of $Q_{\text{He}}=7$ L/min. Installing a single copper ring

electrode on the glass cylinder end and connecting it to the high voltage (HV) source causes the ring electrode and helium gas to interact (the discharge process). Due to the glass dielectric and gas flux, only micro-discharge is possible. The former prevents secondary electrons, and the latter regulates the interaction-time of the HV source and the base gas. The slight thermal effects of micro-discharges bring the partial plasma and carrier helium gas temperatures to about 37°C. A sinusoidal HV source with a peak to peak amplitude of $V_{pp}=8$ kV and a frequency of $\nu=50$ kHz is responsible for the electrical discharge. Since this plasma jet has only one electrode, the second (floating) electrode that plays the ground electrode's role is the tooth surface. In the experiment, the distance between the helium probe and the tooth surface was about $d=10$ mm.

Figure 1b shows an ArJ. The ARG structure differs from He-DBDJ as follows. In ArJ, the reactor body (electric discharge zone) is made of quartz and has a high thermal resistance. In addition, unlike the He-DBDJ in which the retaining glass wall between the helium atoms and the high-voltage ring electrode responsible for preventing the secondary electrons' production, in the ArJ, the single needle-shaped electrode at the axis of symmetry of the cylinder is exposed to argon atoms regardless of any obstacle. That is why the secondary electrons' generation from the needle-shaped electrode and more intense electrical discharge is expectable.

Consequently, significant thermal effects (compared to the He-DBDJ) yields [37]. There are two ways to reduce the thermal effects: reducing the high voltage amplitude or increasing the argon gas flux (or both). We think it is more economical to reduce the high voltage range (less argon gas consumption, $Q_{Ar}=4$ L/min). The reactor wall must protect itself from possible thermal damage while adjusting the high voltage range. Quartz is the right choice that meets the latter purpose. The parameters of ArJ applied in this study are a sinusoidal HV source with $V_{pp}=6$ kV and $\nu=50$ kHz. Like the He-DBDJ, the second electrode is the tooth surface (floating electrode) at a distance of $d=10$ mm from the argon probe.

Figure 1c is a schematic of the Air-DBD. Two main reasons justify the presence of this plasma device in the group of cold plasma generators. First, air (the air in the environment we breathe) is a base gas, and it is more cost-effective than devices that use helium or argon gases. Furthermore, the plasma generated by the electrical discharge of air adjacent to the glass tube covering the HV electrode is quiet and free of the momentum transfer caused by the base gas flux. In designing the present study's algorithm, choosing the Air-DBD without gas flux makes it possible to study gas flux's effect on the enamel surface and fluoride uptake by comparing it with two other devices. The parameters of Air-DBD applied in this study are a sinusoidal HV source with $V_{pp}=4$ kV and $\nu=50$ kHz connected to the needle-shaped electrode. Plasma processing was performed by placing the tooth surface 1mm from the surface of the glass tube.

3. Results

We have used the Scanning Electron Microscope (SEM) and Energy-Dispersive X-ray Spectroscopy (EDX) diagnostic tools to study the effect of different plasma species on tooth enamel and subsequent changes in fluoride ion uptake and the Ion-Selective Electrode (ISE) to measure the fluoride ion release.

Since SEM imaging uses a 10 nm gold coating layer on insulating layers such as tooth enamel, it is necessary to pay sufficient attention to the sample surface's cleanliness and dryness. The applied SEM (FEI Nova, NanoSEM, 450) operating parameters are: charge reduction mode, accelerator voltage 10 kV, working distance 4.5 mm, and a set of magnifications including 250, 500, 1000, 2000, 4000, 8000, and 15000.

Figure 2 demonstrates SEM images related to enamel surface treatment with a) Control group, process-free specimen b) Air-DBD c) ArJ d) He-DBDJ. At a glance, the followings are observable:

1- The control sample (Fig. 2a) is distinguishable by observing porous enamel prisms and mineral deposition evidence with natural features (convex curves within hexagonal boundaries).

2- The micron-sized particles in the Air-DBD processed specimen (Fig. 2b) indicate dust particles in the air.

3- Cracks are present in all samples processed by plasma (Fig. 2b, 2c, 2d).

4- The severe damage of hexagonal structures is observable in the samples processed with Air-DBD (Fig. 2b) and ArJ (Fig. 2c).

5- The convex structures exist similar to the control specimen in the case ArJ (Fig. 2c) and different from the control specimen with concave forms in the Air-DBD (Fig. 2b) and He-DBDJ (Fig. 2c) cases.

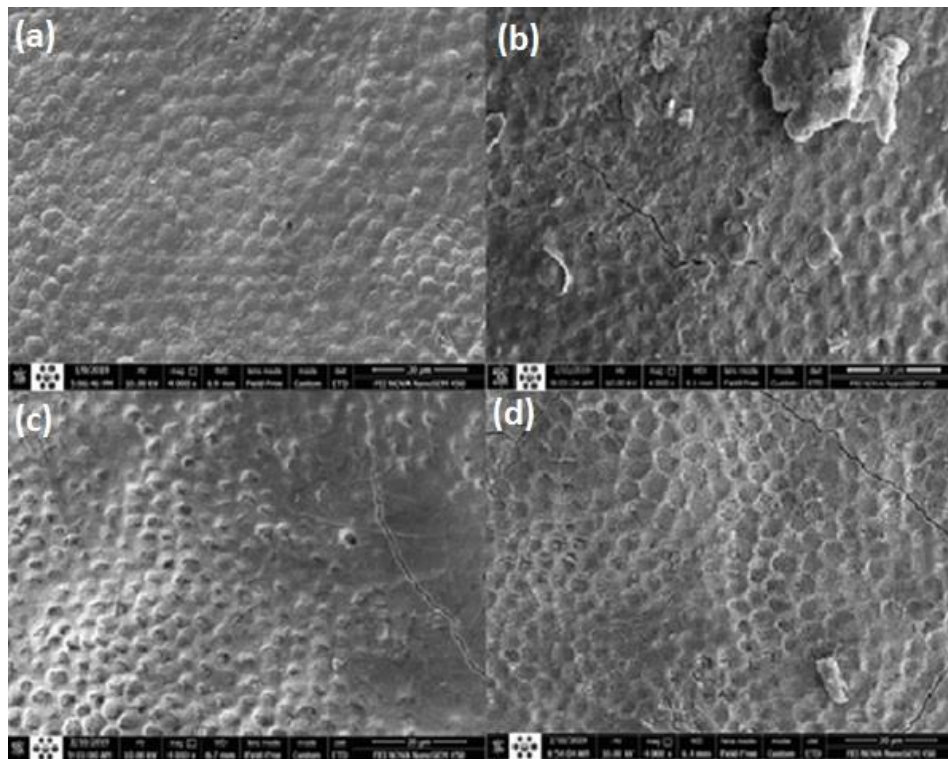


Fig. 2 - SEM images related to enamel surface treatment with a) Control group, process-free specimen b) Air-DBD c) ArJ d) He-DBDJ.

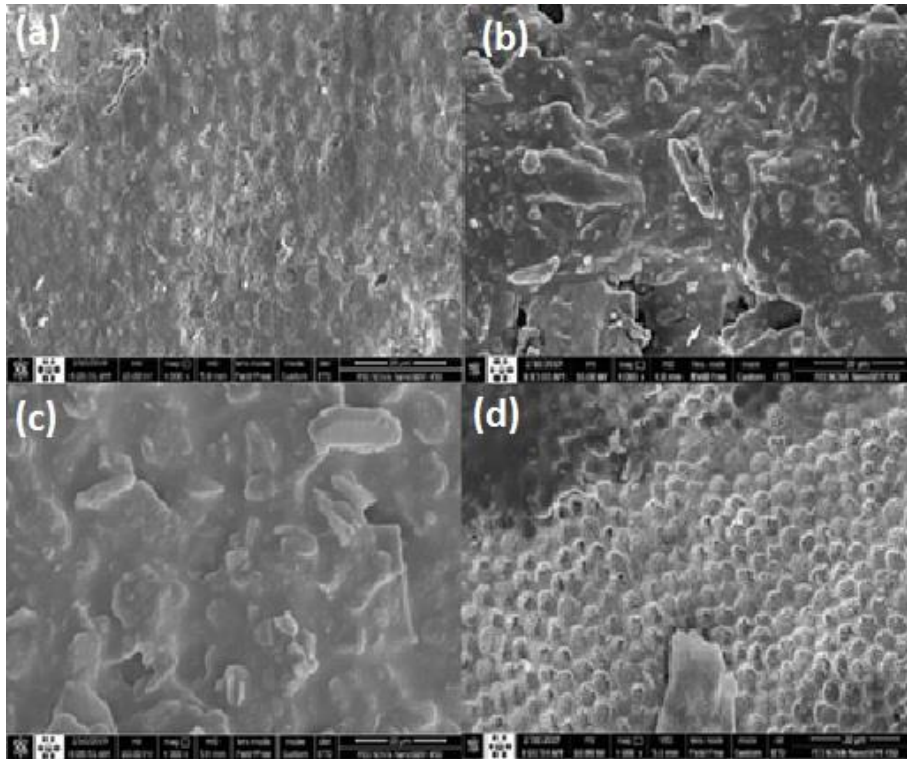


Fig. 3 - SEM images related to enamel surface treatment with a) C+FV b) Air-DBD+FV c) ArJ+FV d) He-DBDJ+FV.

So far, we have reviewed SEM Fig. 2 as qualitative evidence supporting the usefulness of the He-DBDJ application (Fig. 2d) in enamel surface treatment to improve FV's adhesion. What can be seen in SEM Fig. 3 is the evidence that supports the presented hypotheses. Figure 3 demonstrates the processed specimens and the control one after impregnating with FV, as described earlier. The figures' arrangement, representing the control and processed specimens, is the same in SEM Figs. 2 and 3. Figure 3, regardless of the amount of dust mixed with the FV (please see Figs. 3b, Fig. 3c, and Fig. 3d), refers to a floating FV on the surface of Fig. 3b and Fig. 3c specimens. It was expectable because with the destruction of the enamel surface's hexagonal structure, following Air-DBD and ArJ applications, the coefficient of friction of the enamel surface decreased.

Consequently, the adhesion of FV to the surface of the samples decreased. Instead, the control sample and the He-DBDJ processed sample (with a relatively complete hexagonal structure observable in Fig. 2a and Fig. 2d) show recognizable hexagonal structure even after applying the varnish (Fig. 3a and Fig. 3d, emphasizing its greater clarity in Fig. 3d).

As mentioned earlier at the beginning of this section, another diagnostic device used in this connection is EDX. By EDX (BRUKER, XFlash 6, 10), the investigation of elements modification of tooth enamel gets possible. EDX operating parameters are an acceleration voltage of 20 kV and a magnification of 129 times. For this purpose, the window surface of 2×4 mm of the samples were scanned linearly by EDX to measure the specimens' elements using the reflected X-ray. EDX detector analyzes 700 to 1500 counts per second over three 20×20 nm spots. The ratio of calcium to phosphorus is one of the essential quantities in the enamel layer analysis. The larger the ratio, the greater the strength expected for the enamel structure. Emphasizing that we are only reviewing the evidence and postponing the judgment to the point where we have sufficient statistics, let us refer to another evidence that EDX has provided on the ratio of calcium to phosphorus, which can help us summarize the pilot phase. The ratio of calcium to phosphorus in different samples is C+FV 2.3, He-DBDJ+FV 2.42 (in good agreement with the report of Kim *et al.* [39]), ArJ+FV 1.51, and Air-DBD+FV 1.49. What is noteworthy is the consistency of these results with the qualitative analysis based on SEM images' viewing. The ratio of calcium to phosphorus in the two samples processed with ArJ and Air-DBD plasma is lower than the control sample, whereas the one processed by He-DBDJ plasma shows a larger ratio. In the first two, we faced the destruction of some of the hexagonal structures, while in the next two, the most important event was the transformation of the convex hexagonal structure into concave.

The previous paragraph was not the whole story. Figure 4 shows the qualitative analysis of the EDX mapping of fluoride levels. The good news is that, even at a glance, a significant increase in fluoride ions is observable in the sample of He-DBDJ+FV compared to other plasma processed specimens (Air-DBD+FV and ArJ+FV), and especially C+FV.

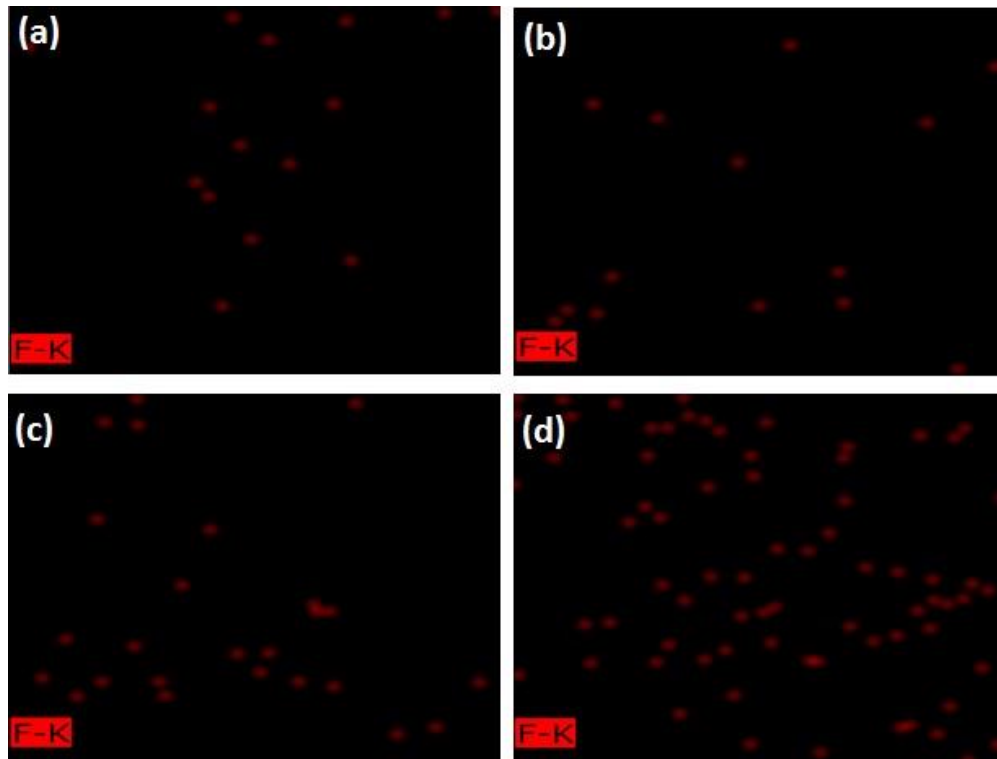


Fig. 4 - EDX mapping allows a qualitative comparison of the number of fluoride ions in tooth enamel between the control sample that received only FV and three other pieces impregnated with FV after various plasma processing. This image is the result of a 20 μ m area scan of enamel. A) C + FV b) Air-DBD + FV c) ArJ + FV d) He-DBDJ + FV.

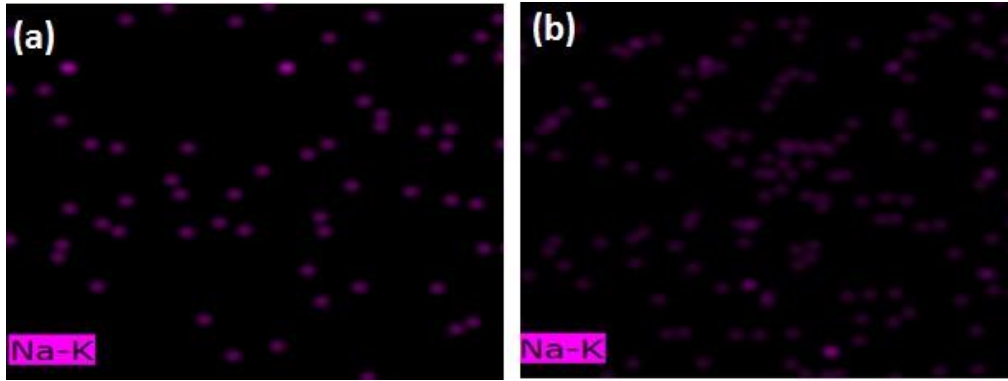


Fig. 5 - EDX mapping allows a qualitative comparison of the amount of sodium in tooth enamel between the control sample that received only FV and the one impregnated with FV after He-DBDJ plasma processing. The image is the result of a 2\$ nm enamel scan area. a) C+FV b) He-DBDJ+FV.

Another considerable evidence in the EDX mapping analysis was sodium presence only in the control specimen and processed by He-DBDJ plasma (please see Figure 5). We know that the source of this sodium is the FV. Nevertheless, what is interesting, and we still have no idea how to explain it, is the absence (at least in the range of used EDX accuracy) of sodium in specimens processed by the Air-DBD and ArJ plasmas.

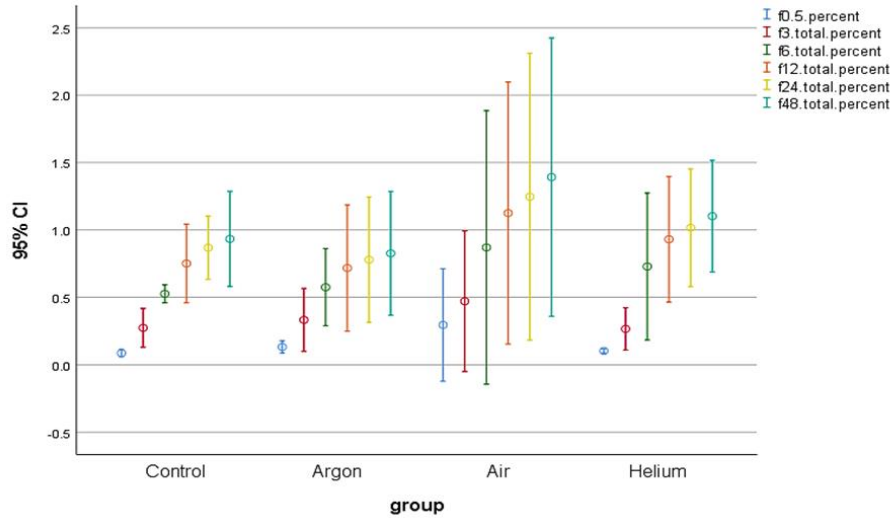


Fig. 6 - Investigation of the effect of plasma processing on the release of fluoride ions from FV. Ion meters measure the fluoride ions release at 0.5, 3, 6, 12, 24, and 48 hours.

The group's dental experience indicated that the degree of fluoride ion uptake from the FV is a measure of the FV quality. Accordingly, whether radicals generated by plasma processing affect the uptake of fluoride ions from the FV is somehow justified. We used an ion-selective electrode (ISE) connected to an ion meter for the fluoride analysis released from FV to aqueous solutions. At this stage, three samples of each subgroup of group B are immersed in individual falcon containers with 25 ml of distilled water at 37°C to check the ion meter's uptake of fluoride ions system (781 PH/Ion Meter, Metrohm). For the fluoride ion uptake calculation, we measure the weight of FV. To this end, it is enough to get the enamel slabs' weight at the beginning and end of the time interval. Therefore, each sample's weight was measured three times according to the standard introduced by (Company, Japan A\$&\$D) with an accuracy of 0.0001 g.

When measuring fluoride, after removing each sample from the storage container and before weighing it, we must clean it from the storage solution attached to it at 4°C. After weighing the sample, transfer it to a new container with 25 ml of fresh distilled water for the next measurement step. As described, the ion meter measures the absorption of fluoride ions at 0.5, 3, 6, 12, 24, and 48 hours after plasma processing. The usual

prescription to control pH and prevent fluoride complexes' formation adds a total ionic strength adjustment buffer (TISAB). The result is a mixture of 20 ml of storage solution, 10 ml distilled water, and 10 ml of acetic buffer solution (TISAB IV, Metrohm, Ion Meter Switzerland). The fluoride concentrations measurement device is a calibrated fluoride-specific electrode (Separate electrode 6.0502.150; Metrohm) attached to an ion meter to an accuracy of 0.001 ppm. The calculated results are the fluoride number up taken per unit area of the sample in mg/cm^2

Figure 6 is the result of the above experiment. The results do not show a significant change. Despite what Figure 6 confirms, it is still too early to judge plasma-derived radicals' effectiveness on the ion uptake process. Accordingly, we hope to activate mechanisms that maximize fluoride ions' maximal absorption by modifying the test method, such as processing plasma FV before applying it to tooth enamel.

4. Discussion

It is necessary to explicitly emphasize that according to the number of dental specimens and the statistics extracted from them, we cannot judge and present a final verdict at all. The purpose of the pilot phase is, as usual, to find evidence to support the idea. Based on the evidence obtained, more extensive tests and more diagnostic tools will be on the agenda. In this way, we hope to finally achieve more credible statistics and other aspects of this issue.

With sufficient caution, it may be possible to link the presence of cracks to plasma processing. Because it is visible in all processed samples but not in the control sample. However, what we have at this stage does not allow us to judge cracks before plasma processing. Nevertheless, if this is the case, it could be due to the transfer of momentum of the plasma particles to the enamel crystal or the fields' interaction around the discharge produced radicals with the enamel layer. The particles' momentum has a transition part supplied by the carrier gas flux and another part due to the acceleration of charged particles in the HV field. The latter has a random velocity distribution due to collisions with other particles that often occur at atmospheric

pressure. We know that the enamel mass does not have a homogeneous structure (that if it did, it would be better to use the word enamel crystal instead). In fact, it consists of several different crystals (such as hydroxyapatite, fluorapatite, different types of Hydroxycarbonate apatite), which stuck together. The bonding forces within crystal constituents are far more substantial than the forces that hold various crystals together. Accordingly, the enamel layer's weakness is the heterogeneity boundaries (the typical boundaries of two or more crystalline species). The most likely place for cracks to form and spread is in a heterogeneous area-the neighborhood of two different crystals (See Ref. [38] for a research study on enamel cracks).

Significant erosion of the enamel surface in both Air-DBD and ArJ reinforces the hypothesis that the carrier gas flux cannot be considered a substantial factor in the erosion process. Because of $Q_{He} > Q_{Ar}$ and $Q_{Air} = 0$. The main agent's search makes accurate spectroscopy of a distance of one centimeter from the He-DBDJ, ArJ, and one millimeter from the Air-DBD inevitable. Adequate knowledge of the different types of radicals produced and their populations will significantly contribute to deciphering the erosion factors. However, even with this amount of information, it can be assumed that the atomic mass of carrier gases has a meaningful relationship with the amount and manner of erosion. Since the highest amount of enamel surface destruction in Air-DBD ($m_{O_2} = 31.998$, $m_{N_2} = 28.014$) and then ArJ ($m_{Ar} = 39.948$) and finally the least that has occurred by converting convex structures to concave in He-DBDJ ($m_{He} = 4.002602$). Whether these gases themselves directly change the enamel surface after ionization or produce a chain of oxygen and nitrogen radicals should be left to post-spectroscopy.

In our opinion, Fig. 2d, which is related to He-DBDJ, demonstrates the most crucial favorable evidence for plasma processing of the enamel surface. The mentioned process with the least destructive and erosive effects on the enamel layer and converting convex structures into concave structures has provided a suitable FV substrate. We emphasize this point in more detail in analyzing the results obtained from FV's use on the four dental specimens shown in SEM Fig. 3.

In fig. 3., To explain the greater clarity, note that in the control sample, due to convex hexagonal structures, we expect less adhesion for the varnish than in the case where the concave hexagonal structure hosts the FV. Therefore, the surface processed by He-DBDJ appears to have a greater capacity to absorb the varnish than the control sample's surface. This factor is a positive point for varnish therapy. Kim *et al.* [39] report a similar conclusion, which is, of course, limited to comparing the He-DBDJ processed sample with the control one.

What is noteworthy in Fig. 4 is the consistency of these results with the qualitative analysis based on SEM images' viewing. The ratio of calcium to phosphorus in the two samples processed with ArJ and Air-DBD plasma is lower than the control sample, whereas the one processed by He-DBDJ plasma shows a larger ratio. In the first two, we faced the destruction of some of the hexagonal structures, while in the next two, the most important event was the transformation of the convex hexagonal structure into concave.

Sodium presence in the EDX mapping analysis is very noticeable. The presence of sodium can temporarily increase local pH. The temporary increase in pH provides the conditions for the chemical reaction of calcium and phosphate ions in the enamel and calcium phosphate formation on the tooth surface. As this process continues, the layer is converted to hydroxycarbonate apatite, structurally and chemically similar to biological apatite [40]. In other words, the presence of sodium activates mechanisms that play a beneficial role for the enamel layer by forming hydroxycarbonate apatite. Figure 5 shows that the amount of sodium in the He+FV sample is higher than in the C+FV sample. Therefore, in terms of the presence of sodium and its subsequent mechanisms, it seems that performing FV after processing enamel with He-DBDJ plasma will be more effective than other techniques in this study.

Putting together the puzzle pieces we have found so far reinforces the idea that if plasma processing increases the FV absorption in the enamel layer, He-DBDJ is the best choice among the plasma devices used in this study.

Although the ion release results do not show a significant change, it is still too early to judge. Still, we hope to activate mechanisms that result in the maximal release of fluoride ions by processing plasma FV before applying it to tooth enamel.

Conclusion

Within the limitations the present study, the following conclusions may be drawn:

1. Although SEM images indicated that Air-DBD and ArJ damaged the hexagonal structure of sample, He-DBDJ was not induced significant morphology change on these dental substrates.
2. He-DBDJ+FV significant increase in fluoride ions in the sample of compared to other plasma processed specimens
3. The ion release results do not show a significant change in compared groups.

Acknowledgments

This research was supported by Dental Research Center of Tehran University of Medical Sciences (TUMS), Tehran, Iran. The authors declare no potential conflicts of interest with respect to the authorship and/or publication of this article.

Author Contributions

Sara. Fathollah, contributed to conception and design, data acquisition, analysis, and interpretation, draft manuscript; Hossein. Abbasi, contributed to conception and design, data analysis, and interpretation, draft manuscript; Mohammad Sadegh Ahmad. Akhondi, contributed to conception and design, data analysis, and interpretation, critically revised the manuscript; Abootorab. Naeemabadi, contributed to design, data acquisition, and interpretation, critically revised the manuscript; Sahar. Emamjome, contributed to design, data acquisition, and analysis, critically revised the manuscript. All authors gave final approval and agree to be accountable for all aspects of the work.

References

- [1] Petersen PE, Bourgeois D, Ogawa H, Estupinan-Day S, Ndiaye C. The global burden of oral diseases and risks to oral health. *Bulletin of the World Health Organization*. 2005;83:661-9.
- [2] Pinkham JR. *Pediatric dentistry infancy through adolescence*: Elsevier Saunders; 2005.
- [3] Featherstone JD. Dental caries: a dynamic disease process. *Australian dental journal*. 2008;53:286-91.
- [4] LeGeros RZ. Calcium phosphates in oral biology and medicine. *Monographs in oral sciences*. 1991;15:109-11.
- [5] Mann A, Dickinson M. Nanomechanics, chemistry and structure at the enamel surface. *Monographs in oral science*. 2006;19:105.
- [6] Azarpazhooh A, Main PA. Pit and fissure sealants in the prevention of dental caries in children and adolescents: a systematic review. *Journal of the Canadian Dental Association*. 2008;74:171-8.
- [7] Rozier RG. Effectiveness of methods used by dental professionals for the primary prevention of dental caries. *Journal of dental education*. 2001;65:1063-72.
- [8] Ahmed AA. Fluoride in Quaternary groundwater aquifer, Nile Valley, Luxor, Egypt. *Arabian Journal of Geosciences*. 2014;7:3069-83.
- [9] Featherstone JD. Prevention and reversal of dental caries: role of low level fluoride. *Community dentistry and oral epidemiology*. 1999;27:31-40.
- [10] Mehta A. Biomarkers of fluoride exposure in human body. *Indian Journal of Dentistry*. 2013;4:207-10.
- [11] Hamilton IR. Biochemical Effects of Fluoride on Oral Bacteria. *Journal of Dental Research*. 1990;69:660-7.
- [12] Adair SM. Evidence-based use of fluoride in contemporary pediatric dental practice. *Pediatric dentistry*. 2006;28:133-42.
- [13] Harris NO, Garcia-Godoy F. *Primary preventive dentistry*: Upper Saddle River, NJ: Pearson Education; 2004.
- [14] Murakami C, Bönecker M, Corrêa MSNP, Mendes FM, Rodrigues CRMD. Effect of fluoride varnish and gel on dental erosion in primary and permanent teeth. *Archives of Oral Biology*. 2009;54:997-1001.
- [15] O Mullane D, Baez R, Jones S, Lennon M, Petersen P, Rugg-Gunn A, et al. Fluoride and oral health. *Community dental health*. 2016;33:69-99.
- [16] Paula ABP, Fernandes AR, Coelho AS, Marto CM, Ferreira MM, Caramelo F, et al. Therapies for White Spot Lesions—A Systematic Review. *Journal of Evidence Based Dental Practice*. 2017;17:23-38.
- [17] Featherstone JDB, Barrett-Vespe NA, Fried D, Kantorowitz Z, Seka W. CO₂ Laser Inhibition of Artificial Caries-like Lesion Progression in Dental Enamel. *Journal of Dental Research*. 1998;77:1397-403.

- [18] Miller E, Vann J, William. The use of fluoride varnish in children: a critical review with treatment recommendations. *Journal of Clinical Pediatric Dentistry*. 2008;32:259-64.
- [19] Xhemnica L, Sulo D, Rroço R, Hysi D. Fluoride varnish application: a new prophylactic method in Albania. Effect on enamel carious lesions in permanent dentition. *European journal of paediatric dentistry*. 2008;9:93.
- [20] Yang G, Lin J-H, Wang J-H, Jiang L. [Evaluation of the clinical effect of fluoride varnish in preventing caries of primary teeth]. *Hua Xi Kou Qiang Yi Xue Za Zhi*. 2008;26:159-61.
- [21] Azevedo DT, Faraoni-Romano JJ, Derceli JdR, Palma-Dibb RG. Effect of Nd: YAG laser combined with fluoride on the prevention of primary tooth enamel demineralization. *Brazilian dental journal*. 2012;23:104-9.
- [22] Rios D, Magalhães AC, Machado MAdAM, da Silva SMB, Lizarelli RdFZ, Bagnato VS, et al. In Vitro Evaluation of Enamel Erosion After Nd:YAG Laser Irradiation and Fluoride Application. *Photomedicine and Laser Surgery*. 2009;27:743-7.
- [23] Souza-Gabriel A, Colucci V, Turssi C, Serra M, Corona S. Microhardness and SEM after CO2 laser irradiation or fluoride treatment in human and bovine enamel. *Microscopy Research and Technique*. 2010;73:1030-5.
- [24] El Sayed I, Abou El Magd D, El Baz G. Effects of ozone on fluoride uptake in enamel. *Egypt Dent J*. 2007;53:1423-30.
- [25] Kalnina J, Care R. Prevention of occlusal caries using a ozone, sealant and fluoride varnish in children. *Stomatologija*. 2016;18:26-31.
- [26] Baptista A, Kato IT, Prates RA, Suzuki LC, Raele MP, Freitas AZ, et al. Antimicrobial photodynamic therapy as a strategy to arrest enamel demineralization: A short-term study on incipient caries in a rat model. *Photochemistry and photobiology*. 2012;88:584-9.
- [27] d'Agostino R, Favia P, Oehr C, Wertheimer MR. Low-temperature plasma processing of materials: past, present, and future. *Plasma Processes and Polymers*. 2005;2:7-15.
- [28] Fathollah S, Mirpour S, Mansouri P, Dehpour AR, Ghoranneviss M, Rahimi N, et al. Investigation on the effects of the atmospheric pressure plasma on wound healing in diabetic rats. *Scientific Reports*. 2016;6:19144.
- [29] Kalghatgi SU, Fridman G, Cooper M, Nagaraj G, Peddinghaus M, Balasubramanian M, et al. Mechanism of Blood Coagulation by Nonthermal Atmospheric Pressure Dielectric Barrier Discharge Plasma. *IEEE Transactions on Plasma Science*. 2007;35:1559-66.
- [30] Keidar M, Shashurin A, Volotskova O, Ann Stepp M, Srinivasan P, Sandler A, et al. Cold atmospheric plasma in cancer therapy. *Physics of Plasmas*. 2013;20:057101.
- [31] Laroussi M. Nonthermal decontamination of biological media by atmospheric-pressure plasmas: review, analysis, and prospects. *IEEE Transactions on Plasma Science*. 2002;30:1409-15.
- [32] Hong Q, Dong X, Chen M, Xu Y, Sun H, Hong L, et al. Disinfection of *Streptococcus mutans* biofilm by a non-thermal atmospheric plasma brush. *Japanese Journal of Applied Physics*. 2016;55:07LG2.

- [33] Lehmann A, Rueppell A, Schindler A, Zylla IM, Seifert HJ, Nothdurft F, et al. Modification of enamel and dentin surfaces by non-thermal atmospheric plasma. *Plasma Processes and Polymers*. 2013;10:262-70.
- [34] Naujokat H, Harder S, Schulz LY, Wiltfang J, Flörke C, Açil Y. Surface conditioning with cold argon plasma and its effect on the osseointegration of dental implants in miniature pigs. *Journal of Cranio-Maxillofacial Surgery*. 2019;47:484-90.
- [35] Wang J, Yang X, Sun K, Sun P, Pan J, Zhu W, et al. Tooth Enamel Evaluation After Tooth Bleaching With Hydrogen Peroxide Assisted by a DC Nonthermal Atmospheric-Pressure Plasma Jet. *IEEE Transactions on Plasma Science*. 2012;40:2157-62.
- [36] Wu C-C, Wei C-K, Ho C-C, Ding S-J. Enhanced Hydrophilicity and Biocompatibility of Dental Zirconia Ceramics by Oxygen Plasma Treatment. *Materials*. 2015;8.
- [37] Schutze A, Jeong JY, Babayan SE, Park J, Selwyn GS, Hicks RF. The atmospheric-pressure plasma jet: a review and comparison to other plasma sources. *IEEE transactions on plasma science*. 1998 Dec;26(6):1685-94.
- [38] Beniash E, Stifler CA, Sun CY, Jung GS, Qin Z, Buehler MJ, Gilbert PU. The hidden structure of human enamel. *Nature communications*. 2019 Sep 26;10(1):1-3.
- [39] Kim YM, Lee HY, Lee HJ, Kim JB, Kim S, Joo JY, Kim GC. Retention improvement in fluoride application with cold atmospheric plasma. *Journal of dental research*. 2018 Feb;97(2):179-83.
- [40] Gjorgievska, E.S. and J.W. Nicholson, A preliminary study of enamel remineralization by dentifrices based on RECALDENT™ (CPP-ACP) and Novamin®(calcium-sodium-phosphosilicate). *Acta Odontologica Latinoamericana*, 2010. 23(3): p. 234-239.